Downstream process and evaluation of the concomitant impact of a recombinant glycosylated L-asparaginase on leukemic cancer cells and the bone marrow tumor microenvironment

Process Biochemistry 131 (2023) 41–51

Contents lists available at ScienceDirect

Process Biochemistry

journal homepage: www.elsevier.com/locate/procbio

Downstream process and evaluation of the concomitant impact of a recombinant glycosylated L-asparaginase on leukemic cancer cells and the bone marrow tumor microenvironment

Eduardo Krebs Kleingesinds [a,*], Letícia de Almeida Parizotto [b], Brian Effer [c], Gisele Monteiro [a], Paul F. Long [d], Yoana Arroyo-Berdugo [e], Volker Behrends [e], Maria Teresa Esposito [e], Yolanda Calle [e,**,1], Adalberto Pessoa-Jr [a,1]

[a] Departamento de Tecnologia Bioquímico-Farmacêutica, Faculdade de Ciências Farmacêuticas, Universidade de São Paulo, 05508–000 São Paulo, SP, Brazil
[b] Departamento de Engenharia Química, Escola Politécnica, Universidade de São Paulo, 05508–000, São Paulo, SP, Brazil
[c] Center of Excellence in Translational Medicine (CEMT) and Scientific and Technological Bioresource Nucleus (BIOREN), Universidad de La Frontera, Temuco, Chile
[d] Institute of Pharmaceutical Sciences, King's College London, SE1 9NH London, United Kingdom
[e] School of Life and Health Sciences, University of Roehampton, London SW15 4JD, United Kingdom

ARTICLE INFO

Keywords:
L-ASNase
Leukemia
Pichia pastoris
Protein purification
Cross-flow filtration
Tumour microenvironment

ABSTRACT

L-asparaginase (L-ASNase) is a life-saving medication used in the treatment of Acute Lymphoblastic Leukemia (ALL) which affects over 60,000 people yearly. However, L-ASNase still requires improvement since up to 60% of the patients develop hypersensitivity due to its immunogenicity. To address this issue, this work describes the downstream process of an L-ASNase from *Erwinia chrysanthemi* expressed extracellularly by *Pichia pastoris* with human-like glycosylation pattern and its further impact on leukemic cells co-cultured with bone marrow (BM) cytoprotective stromal cells. After size exclusion chromathography, a final yield of 54.93% was achieved and the proteomics analyses confirmed the attainment of an extremely pure enzyme. Glycosylated L-ASNase induced the complete inhibition of the proliferation of ALL and Acute Myeloid Leukemia (AML) cell lines tested, independently of the presence of BM stromal cells. However, the cytotoxic efficacy (induction of apoptosis) of glycosylated L-ASNase varied across cell lines, with ALL cell lines showing the most sensitivity. Additionally, the pro-apoptotic effect of glycosylated L-ASNase was partially inhibited by BM stromal cells. Taken together, our data warrant further investigations for the use of glycosylated L-ASNase against ALL and AML that should take into consideration the mechanisms of resistance mediated by the BM stroma for improved efficacy.

1. Introduction

Acute Lymphoblastic Leukemia (ALL) represents the most frequently diagnosed leukemia in children and young adults (90%) [1,2]. ALL arise in the bone marrow where normal hematopoietic cells are hijacked by immature lymphoid leukemic cells, resulting in decreased erythrocyte and platelet counts [3,4]. As a result, patients develop anemia and can experience symptoms such as fatigue, pallor, higher vulnerability to infections, and bleeding episodes. ALL can arise in either B-cell (B-ALL) or T-cell (T-ALL) progenitors and can affect both children and adults. While the outcome of pediatric B-ALL patients has drammatically improved over the past 15 years with survival rates reaching 80% at 5 years, the prognosis of the adult B-ALL patients is much worse and the survival rate reaches only 50–60% [1–3]. This is at least in part due to the fact that adult patients express the BCR::ABL1 fusion protein. Chemoresistance and relapse of acute leukemia are due to a pool of leukemic stem cells (LSC), a heterogeneous group of cells responsible for initiating and maintaining the disease [4]. While current treatments are effective against the buk of the ALL tumour, they do not eradicate the LSC. These therapy surviving leukemia, also known as minimal residual disease

* Correspondence to: Process and Systems Engineering Center (PROSYS). Technical University of Denmark Dept. of Chemical and Biochemical Engineering, Lyngby, Denmark.
** Corresponding author.
E-mail addresses: eduklei@dtu.dk (E.K. Kleingesinds), yolanda.calle-patino@roehampton.ac.uk (Y. Calle).
[1] These authors contributted equally to this work.

https://doi.org/10.1016/j.procbio.2023.06.006
Received 11 January 2023; Received in revised form 10 May 2023; Accepted 5 June 2023
Available online 7 June 2023

(MRD) determines the relapse of leukemia [3]. Several mechanisms contribute to the survival of these highly refractory LSC, including the protection provided by mesenchymal stromal cells and other cells including adypocytes, T and B cells, dendritic cells, and macrophages, in the bone marrow (BM) microenvironment which works as a sanctuary where leukemic blasts and LSC can acquire a drug-resistant phenotype and evade the treatment [4–6].

Among the main therapies used to treat ALL is L-Asparaginase (L-ASNase) (EC 3.5.1.1, L-Asparagine amidohydrolase). Its mode of action consists of a starving mechanism where L-asparagine (Asn) and L-glutamine (Glu) are depleted from blood and BM [7]. Since leukemic blasts are deficient in expression levels of the asparagine synthetase gene (ASNS) (EC 6.3.5.4), neoplastic cells become dependent on Asn from the bloodstream. Depravation of these two amino acids leads to the inhibition of overall constitutive protein synthesis and the leukemic cells undergo apoptosis [2]. On the other hand, healthy cells are self-sufficient in the production of this amino acid and are not affected by the action of L-ASNase [8].

Improving the efficacy of L-ASNase-based treatment will require addressing some remaining challeges in the currently available L-ASNase formulations such as the side effects caused by impurities or by silent inactivation by the immune system. Additionally, according to Patel and collaborators (2009) [9] therapy failure is caused by the inactivation of L-ASNase by cellular lysosomal cysteine proteases. It is important to pinpoint that microenvironmental cells, such as macrophages, can produce cathepsin B (CTSB) and contribute to ASNase turnover in vivo in mice [4,10].

The available commercial L-ASNases approved by the FDA for therapeutic purposes have been sourced from bacteria (*E. coli* and *E. chrysanthemi*) [2]. However, the administration of these exogenous proteins may induce an immune response, leading to the production of anti-asparaginase antibodies. This is the main cause of reduced drug efficacy, resulting from reduced L-ASNase activity and undesirable effects such as pancreatitis, coagulation disorders, and diabetes [11,12].

To overcome these side effects, a few studies have reported chemical modifications such as encapsulation [13] and PEGylation (where the enzyme is covalently bound to polyethyleneglycol (PEG)) [14,15]. These modifications reduce the immunogenicity of the molecule by masking the epitopes that otherwise activate the immune system. Moreover, the polymer stabilizes the enzyme and increases its half-life. However, the only chemical modification approved to date by the FDA for L-ASNase for human use is the PEGylated version [11].

While chemical reactions can improve biopharmaceuticals in terms of stability and immunogenicity, the PEGylation reaction can also be emulated through a biological route, exploring the tools from the recent trends that molecular biology had brought. More specifically, a great attention has been drawn towards exploiting the potential of post-translational modifications, such as glycosylation, in new biotherapeutics. Glycosylated proteins are covered with oligosaccharides, which, similarly to pegylation, provide stability and correct folding, and may influence both their cellular activity and their biological function [16]. Oligosaccharides may be bound to the Asn residues to form the N-glycans (which is more common), or to the threonine or serine residues, forming O-glycans [17]. This tends to decrease adverse reactions such as those observed with the use of L-ASNases from bacterial sources [11].

Yeasts had become a valuable host system for the expression of recombinant proteins as they are eukaryotic organisms able to perform glycosylation. Among them, the most well known systems to express recombinant proteins are *Saccharomyces cerevisiae* and *Pichia pastoris*. However, contrary to mammalian cells, protein glycosylation in microorganisms results in high-mannose N-glycans that may cause immunogenic reactions when interacting with human mannose receptors present in immune cells, which results in rapid clearance from the bloodstream [18].

To overcome these limitations, the possibility of reengineering the N-glycosylation pathway in yeast to obtain glycoproteins with human-like pattern has become a promising approach among biochemical processes [18,19]. One advantage of using the methylotrophic yeast *P. pastoris* machinery rather than *S. cerevisiae* lies in the fact that the levels of hyperglycosylation in *P. pastoris* were found to be much lower (approximately 50 residues) than in *S. cerevisiae* (~500 residues) [18]. When engineered, *P. pastoris* adds 5 residues of mannose in the final oligosaccharide.

The anti-leukemic effect of L-ASNase has been extensively investigated in ALL, but only partially in Acute Myeloid leukemia (AML) [4]. AML is a heterogeneous blood cancer and represents the most frequently diagnosed leukemia in adults (25%) and accounts for 15–20% cases in children [3]. Despite continuous advances in the comprehension of AML prognosis, patients are still subject to a high rate of relapse [3].

Some specific subtypes of AML have been reported to be more susceptible to ASNase as compared to others [20–22]. This is due to AML cells present a proclivity addiction in glutamine for their energetic and biosynthetic metabolism [23–25]. Hence, the efficacy of L-ASNase should be considered in future studies targeting AML cells.

According to the literature, co-culture models provide a highly relevant drug screening setting for testing L-ASNase as a possible therapeutic intervention in ALL and AML since the BM tumour stroma has been shown to be the major source for Asn to leukemic blasts [1,4]. By co-culturing mCherry-HS5 BM fibroblastic stromal cells and eGFP-expressing tumour cell lines that frequently originate in the BM, it is possible to evaluate these reciprocal effects on cancer and BM stromal cells. This platform can be scaled up to high throughput using 96 well plates and allows the concomitant assessment of both tumour and BM stroma response to anticancer drugs [26]. Hence, this fluorescent-based co-culture methodology allows the evaluation of the reciprocal effect of the stromal cell and anticancer therapy on tumour cells [26].

As described in a previous study, our research group has constructed a new *P. pastoris* strain (Glycoswitch_pJAG-s1_*asnb*) that can express an active extracellular L-ASNase from *E. chrysanthemi* with human-like glycosylation [27]. The present work presents a critical approach of the downstream processing by crossflow filtration and high-resolution techniques evaluating the final yield of the process and the specific activity of the glycosylated L-ASNase and aimed to investigate its effect on leukemic blasts in the presence of the cytoprotective BM microenvironment.

2. Material and methods

2.1. Expression system

The recombinant *Pichia pastoris* Glycoswitch® Superman5 (his$^-$) strain is being used to carry the *asnB* gene (i.e. amino acid residues 22–348 UniprotKB – P06608) from *E. chrysanthemi*. This construction used the pJAG-s1_*asnB* expression vector as previously described [27]. The L-ASNase is glycosylated and secreted into the cellular medium [11].

2.2. Production of L-ASNase with human-like glycosylation pattern in a bench bioreactor

L-ASNase was produced in bioreactor as described by Parizotto et al., 2021 [28]. Briefly, glycerol was used as a carbon source during the first 24 h of cultivation at batch mode. Once all glycerol had been consumed, the induction phase with methanol began, in which the system was fed with methanol every 24 h. The temperature was maintained at 35 °C throughout the cultivation and aeration was maintained at 1 vvm and initial agitation at 700 rpm and a target value of 20% dissolved oxygen was kept with cascade control of agitation between 700 and 1000 rpm.

2.3. Downstream

2.3.1. Crossflow filtration

To evaluate the purity of the glycosylated L-ASNase obtained by biotechnological route, two strategies were investigated.

Strategy 1: After 24 h of culture induction, a 5 mL sample was collected from the reactor and, after centrifugation (3000 *xg* for 10 min at 4 °C), its activity was measured in the supernatant. Then, the extracellular medium containing L-ASNase was transferred to four 250 mL centrifuge vials each. The medium was then centrifuged at 3000 *xg* for 10 min at 4 °C. After that, the supernatant was redistributed to 50 mL centrifuge vials and centrifuged again at 10000*xg* for 10 min. Finally, the entire collected medium was vacuum filtered on 0.45 μm membrane (Fig. 1).

Strategy 2: After 24 h of culture induction, a 5 mL sample was taken from the reactor and, after centrifugation (3000 *xg* for 10 min at 4 °C), its activity was measured. Then the extracellular medium containing L-ASNase was transferred to four 250 mL centrifuge vials each. The medium was then centrifuged at 3000*xg* for 10 min at 4 °C to separate the medium from the cells. After this time, a 300 kDa cut-off membrane was used to remove the remaining cell debris by tangential ultrafiltration. Thus, the permeate was collected for the next steps (Fig. 1).

Extracellular media from strategies 1 and 2 were separately concentrated and diafiltered using the Sartoflow Slice 200 Benchtop System (120 V) ultrafiltrator (Brand Sartorius® Stedim Biotec) under the following conditions: flow rate of 400 mL min^{-1}; 30 psi of transmembrane pressure; polyethersulfone membrane; and three different pore sizes were studied separately (10, 30 and 100 kDa). The medium was then concentrated tenfold and buffer exchange was performed by the addition of sodium acetate buffer (50 mM, pH 5.2) upon reaching the desired (pH 5.2) to perform the next step of the purification process: the cation exchange chromatography.

2.3.2. Cationic exchange chromatography

A 20 mL SP HP column (GE Healthcare, USA) was used for cation exchange. To equilibrate the column, three column volumes (CV) of sodium acetate buffer (50 mM, pH 5.3 with 100 mM of glycine) were used. The sample was loaded into the column using the Akta Start (GE Healthcare, USA) peristaltic pump with a flow rate of 0.5 mL min^{-1} to ensure that the protein binds with the column resin. Finally, the column was washed with 1.5 column volumes of the same buffer to remove the excess of contaminant proteins. The target protein was eluted with sodium acetate buffer (50 mM, pH 5.3 with 100 mM of glycine) with NaCl 1 M by step mode on the range of 0–100 mM of NaCl 1 M increasing 20 mM of NaCl every 3 CV. Samples of 500 μL were collected to measure enzyme activity, total protein concentration, and purity using SDS-PAGE. The remaining enzyme was purified by gel filtration.

2.3.3. Size-exclusion chromatography

After Cationic Exchange Chromatography, size-exclusion was performed using the Superdex™ 200 Increase 10/300 GL column (GE Healthcare, USA). The column was washed with water and equilibrated with two column volumes of pH 5.5 sodium acetate buffer with 100 mM glycine. The protein was eluted with 1.5 column volumes of the same buffer at a flow rate of 0.75 mL.min^{-1}.

2.3.4. Determination of enzyme activity

Pure enzyme activity was estimated using the modified Nessler method according to Simas et al., 2021 [29], where 1 unit represents the release of 1 μmol ammonia per minute. Briefly, in a 96-well plate, 168 μL Asn (44 mM), 148 μL 50 mM Tris HCl buffer (pH 8.6), 37 μL ultra-pure water, and 17 μL sample were added. After 10 min incubating at 37 °C, the reaction was stopped by adding 17 μL of 1.5 M trichloroacetic acid. In another 96-well plate, 279 μL of ultra-pure water, 37 μL of Nessler's reagent, and 37 μL of the previous reaction were added and the absorbances read at 440 nm in a plate reader SpectraMax (Molecular Devices, USA). The absorbance measurement was then compared to the standard curve previously made with the Nessler reagent and ammonium sulfate at concentrations of 0.05, 0.1, 0.25, 0.5, 1.0, and 2.5 mM.

2.3.5. Polyacrylamide gel electrophoresis (SDS-PAGE)

For SDS-PAGE, 20 μL of samples from each purification step were

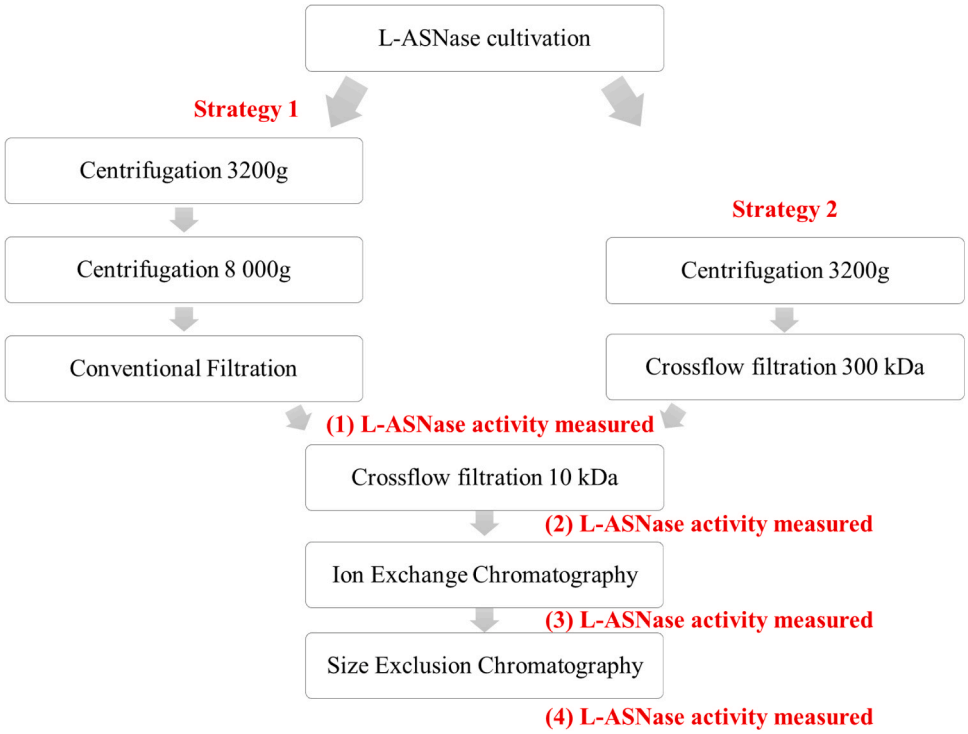

Fig. 1. Schematic diagram of the process purification. On the left, strategy 1 with conventional filtration. On the right, strategy 2 where conventional filtration was replaced by crossflow filtration with a 300 kDa membrane.

transferred to a microtube and 5 μL of Laemmli sample buffer + dithiothreitol (DTT) were added and then heated at 95 °C for 5 min

Using a 12% acrylamide separating gel, samples were loaded into the lanes and the protein marker (BioRad, USA) was loaded into the first and the last lane. The voltage was set to 120 V and the running buffer (tris-glycine pH 8.5 + SDS 1% (w/v) was added until the top of the electrophoresis system. When the run was completed, the polyacrylamide gel was stained with Coomassie Blue R-250 for 1 h, and then it was destained overnight with solution (40 v/v % methanol, 20 v/v % acetic acid).

2.3.6. Total protein assay

Total protein was determined by the BCA (bicinchoninic acid assay) method. Initially, a calibration curve was constructed using BSA (bovine serum albumin) in the range 0.1–1.2 mg mL^{-1}. Then, before measuring the protein concentration, interferences were removed using the Non-Interfering Protein Assay™ (Calbiochem®, USA) kit. A solution of bicinchoninic acid (50 parts) plus copper sulfate (1 part) was prepared for each sample. From this mixture, 200 μL were aliquoted into an Eppendorf tube and 25 μL of the sample were added. After homogenization, it was incubated for 30 min at 37 °C. Finally, the absorbance was measured at 562 nm.

2.3.7. Proteomics analysis by LC-MS/MS

This analysis was performed to asses the final purity of the glycosylated L-ASNase. In-gel reduction, alkylation, and digestion with trypsin (Sigma-Aldrich; Trypsin sequencing grade) was performed on the gel sample prior to the analysis by mass spectrometry. Cysteine residues were reduced with dithiothreitol (10 mM) and derivatized by treatment with iodoacetamide (55 mM) to form stable carbamidomethyl derivatives. Trypsin digestion was carried out overnight at room temperature after initial incubation at 37 °C for 2 h.

The peptide sample was suspended in 30 μL of resuspension buffer (2% acetonitrile (ACN) in 0.05% formic acid (FA)), 10 μL of which were injected to be analyzed by LC-MS/MS. Chromatographic separation was performed using a U3000 UHPLC NanoLC system (ThermoFisher-Scientific, UK). Peptides were resolved by reversed phase chromatography in a 75 μm C18 column (50 cm length) using a three-step linear gradient of 80% ACN in 0.1% FA. The gradient was set to elute the peptides at a flow rate of 250 $nl.min^{-1}$ over 60 min. The eluate was ionized by electrospray ionization using an Orbitrap Fusion Lumos (ThermoFisherScientific, UK) operating under Xcalibur v4.1.5. The instrument was first programmed using a "Universal_CID" method by defining a 3 s cycle time between a full MS scan and MS/MS fragmentation. This method takes advantage of the multiple analyzers on Orbitrap-Fusion-Lumos and drives the system to use all available parallelizable time, resulting in decreasing the dependence on method parameters (such as data dependent acquisition). The instrument was programmed to acquire in the automated data-dependent switching mode, selecting precursor ions based on their intensity for sequencing by collision-induced fragmentation using a TopN CID method. The MS/MS analyses were conducted using collision energy profiles that were chosen based on the mass-to-charge ratio (m/z) and the charge state of the peptide.

2.4. Cell culture

The following Human eGFP-ALL cell lines were used in our experiments: HB-119, SEMK2 and REH. HB-119 and REH were a generous gift of Prof. Eric So (King's College London) and Prof Owen Williams (University College London), respectively. We also evaluated the action of L-ASNase on the eGFP-AML cell line MV4–11. The fibroblastic HS5 cell line transduced with the red fluorescent protein mCherry was used as a source of bone marrow stromal cells [30]. We analyzed eGFP-ALL and eGFP-AML cell proliferation and apoptosis on mCherry-HS5. mCherry-HS5 human stromal cell line were cultured in Dulbecco's modified Eagle medium with L-glutamax supplemented with 10% of fetal bovine serum (FBS). All eGFP-tumour cell lines were cultured in RPMI-1640 medium supplemented with 10% of FBS. All cell lines were cultured at 37 °C in a humidified atmosphere in the presence of 5% of CO2, 95% air.

2.5. Determination of cell proliferation and viability of tumour cells in co-culture with mCherry HS5 cells

mCherry fibroblastic stromal cells were seeded at 5×10^3 cells/per well in a 96-well plate and incubated overnight. eGFP-positive cells were seeded alone or layered on mCherry-HS5 cells in triplicate per condition. We evaluated the effect of drug treatment plus untreated control of eGFP cells seeded alone or in co-culture with BM microenvironment cell after leaving blank wells for calculation of background values. The fluorescence intensity per well was read at λex488 nm/528 nm and at λem584 nm/607 nm to detect the numbers of eGFP tumour cells and mCherry HS5 cells, respectively, using a FLx800 multidetector microplate reader (Biotek Instruments, Potton, Bedfordshire, UK) at day 0 and day 3. The proliferation index was calculated by dividing the fluorescence intensity in the same well at day 3/day0 after subtracting the average of the background values of the corresponding condition (eGFP cultured alone or in co-culture). The various tumour cell lines cultured alone or in co-culture were treated with concentrations of L-ASNase in the range of 0.1–1.0 IU.

2.5.1. Fluorescence microscopy

Cells seeded in 96 well plates were imaged using an Elipse Nikon fluorescence microscope (Nikon UK Limited, Surrey, UK) equipped with a motorised stage and an environmental chamber with controlled temperature and CO_2 levels. Images were captured and exported as JPEG files using NIS-Elements Nikon software.

2.5.2. Flow cytometry analysis

Cell suspensions of cultured cells were prepared at day 3 for fluorescence activated cell sorting (FACS) analysis using a flow cytometer (BD Accuri C6, USA). Analysis of forward scatter (FSS) and side scatter (SC) as well as the levels of emission of fluorescence of eGFP (λexcitation 395 nm; λemission). Data were analysed using the BD Accuri C6 Analysis software.

2.5.3. Intracellular amino acid quantification

Intracellular amino acids from HB-119, REH, and MV411 lineages were measured by UPLC-MS/MS using precolumn derivatization with 6-aminoquinolyl-N-hydroxysuccinimidyl carbamate (AccQTag kit) [31].

3. Results and discussion

3.1. Protein purification

Glycoproteins are promising therapeutical molecules in the biopharmaceutical field. The newly developed glycosylated L-ASNase can be identified by the analysis of the chromatograms shown in Fig. 2.

Even after one single step of cationic exchange chromatography, only one active and well-resolved peak was detected (Fig. 2 A). This can be explained by the first purification steps using crossflow filtration (strategy 2) and because the protein is expressed to the extracellular medium, which simplifies the downstream process and avoids proteins from the intracellular space (that could be immunogenic) to contaminate the product. After size exclusion chromatography (Fig. 2B) a very well-resolved active peak was observed as well as one additional fraction that showed low activity attributable to other proteoforms expressed in smaller amounts. It further showed an active L-ASNase peak eluted in a time corresponding to a 160 kDa protein, which suggests that the enzyme expressed in *P. pastoris Glycoswitch* preserved the original tetrameric configuration of L-ASNase observed in *E. coli* and *E. chrysanthemi*.

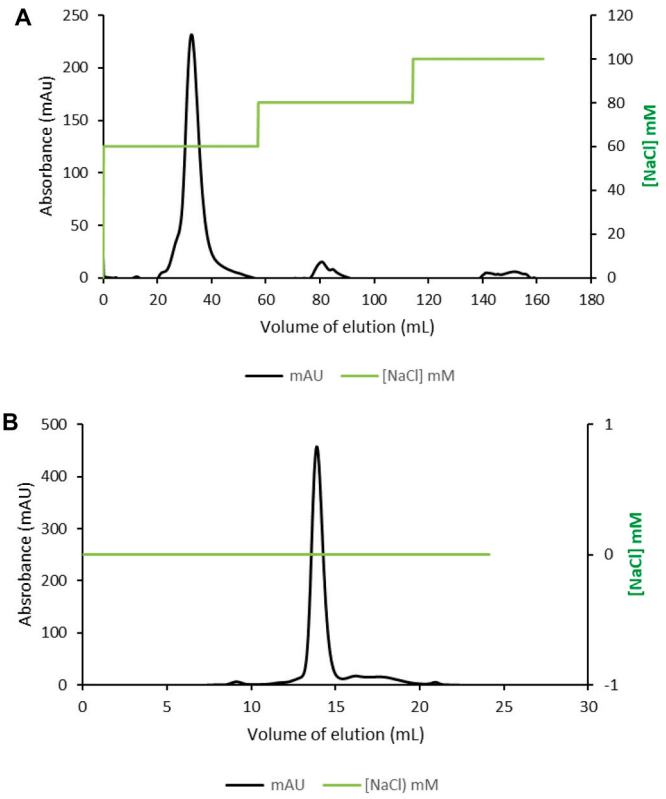

Fig. 2. Chromatograms of glycosylated L-ASNase after cationic exchange chromatography (A) and size exclusion chromatography (B). Elution for cationic exchance chromatography by step gradient mode with sodium acetate buffer (50 mM, pH 5.3 with 100 mM Glycine) and NaCl 1 M (on steps 60 mM, 80 mM, 100 mM). Elution for size exclusion chromatography with sodium acetate buffer (50 mM, pH 5.5 with 100 mM glycine).

Fig. 3 shows the SDS-PAGE throughout the downstream process of our L-ASNase in which the increasingly concentrated and pure 40 kDa band can be observed, which corresponds to the glycosylated L-ASNase monomer. The glycosylated L-ASNase tetramer can be seen in Fig. 2B, corresponding to 160 kDa. Comparing Figs. 2 and 3, it is possible to conclude that the enzyme is more pure after size exclusion chromatography.

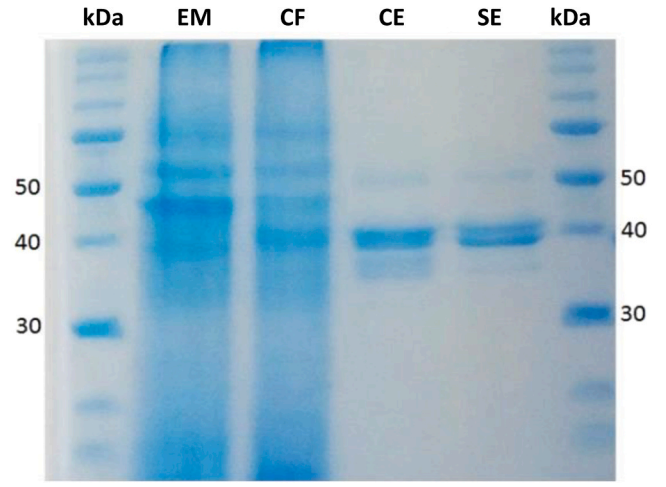

Fig. 3. SDS-PAGE of glycosylated L-ASNase from each purification step: Extracellular Medium (EM); Crossflow filtration (CF); Cationic Exchange chromatography (CE); Size exclusion chromatography (SE).

3.2. Evaluation of the purity of the glycosylated L-ASNase by LC-MS/MS

In our previous work, we have analyzed the L-ASNase presented in this research through mass spectrophotometry. We have found that this L-ASNase is glycosylated in the epitope ASN_{170} with the glycan $GlcNAc_2Man_7$ [11].

It is well known that injectable biopharmaceuticals must have a very high purity degree to avoid undesirable side effects. From the regulatory perspective, impurities can be process related (host cell proteins, media residues, column leachables) or product related (precursors, degradation products, aggregates). Understanding the impurities is essential to developing control strategies to reduce or remove them from the final product [32]. Thus, to provide an extensive information about the purity of our L-ASNase after our downstream process, we performed proteomic analysis by LC-MS/MS to identify potential remaining contaminants. Table 1 shows the results of proteomics of the glycosylated L-ASNase after the purification process.

Given the absence of contaminating proteins in the final purified fraction, we can conclude that our process yielded an extremely pure protein after downstream processing. The contaminants detected by the proteomic analysis are from the sample preparation. Recently, Zenatti and collaborators [33] performed a similar analysis by LC-MS/MS of the impurities from the two L-ASNases available in the Brazilian market used to treat ALL. Their findings had shown a very high amount of impurities in Leuginase® in contrast to the impurities from Aginasa® [33]. Therefore, our purification process is significantly better than the ones currently used for commercial production, having potential for scale-up and eventually reaching market after clinical trials.

3.3. Evaluation of the downstream yield of the glycosylated L-ASNase

While biopharmaceutical product purity is a critical criteria in process development, the process yield is just as relevant in the industrial production setting. Hence, we evaluated the L-ASNase yield and enrichment after each step of the downstream process, (Tables 2A and 2B), for the two purification strategies tested.

In view of a possible loss resulting from the use of the filter in conventional filtration (strategy 1), we decided to change the clarification steps prior to crossflow filtration. Thus, centrifugation and conventional filtration were excluded and crossflow filtration with a 300 kDa cut-off membrane was adopted (strategy 2). Since the protein was approximately 140–160 kDa, using strategy 2, we first collected the permeate from this step, and then this permeate went through crossflow filtration using a 10 kDa cassette.

A loss of approximately 28% of the enzyme activity and a yield of 72.08% were detected after strategy 1 (the use of the filter in conventional filtration), while strategy 2 resulted in 98.20% recovery of the enzyme (Tables 2A and 2B). In both cases, the enzyme is unlikely to have been lost to the permeate since it did not present detectable L-ASNase activity and the molecular weight of the enzyme is over one order of magnitude larger than the 10 kDa membrane pore-size.

It is noteworthy that the clarification steps prior to crossflow filtration are necessary because we need to ensure complete removal of cells from the extracellular medium (where L-ASNase is contained) to avoid column clogging in the later stage of cation exchange chromatography. The overall yield of the purification processes were 39.31% and 54.93%

Table 1
Proteins identified by LC-MS/MS analyses from L-ASNase with human-like glycosylation pattern expressed extracellularly by recombinant *Pichia pastoris* after protein purification.

Accession	Identified protein	Spectral peptides count	kDa
ASPG_DICCH	L-Asparaginase	212	38
TRY1_BOVIN	Cationic trypsin	18	26
ACTB_XENLA	Cluster of actin	8	42

Table 2A
– Purification process of L-ASNase with human-like glycosylation pattern expressed extracellularly by recombinant *Pichia pastoris* using a 10 kDa cassette during crossflow filtration (strategy 1).

Purification steps	Volume (mL)	Activity (U/mL)	[Total Proteins] mg/mL	Total Activity (IU)	Total Proteins (mg)	Specific Activity (U/mg)	Purification fold	Yield (%)
(1) Extracellular Medium	700.0	1.5	0.3	1014.6	178.3	5.7	1.0	100.0
(2) Crossflow filtration and diafiltration	140.0	5.2	0.3	731.3	45.9	15.9	2.8	72.1
(3) Cationic exchange chromatography	1.3	332.9	2.6	416.1	3.3	128.0	22.5	41.0
(4) Size exclusion chromatography	1.5	265.9	1.1	398.9	1.6	253.3	44.5	39.3

Table 2B –
Purification process of L-ASNase with human-like glycosylation pattern expressed extracellularly by recombinant *Pichia pastoris* using a 300 kDa cassette before the 10 kDa cassette during crossflow filtration (strategy 2).

Purification steps	Volume (mL)	Activity (U/mL)	Total Proteins mg/mL	Total Activity (IU)	Total Proteins (mg)	Specific activity (U/mg)	Purification fold	Yield (%)
(1) Extracellular medium	500.0	3.5	0.5	1743.5	260.3	6.7	1	100
(2) Cross flow filtration and diafiltration	85.0	20.1	1.0	1712.1	87.3	19.6	2.9	98.2
(3) Cationic Exchange Chromatography	1.8	539.5	1.8	987.3	3.2	307.1	45.9	56.6
(4) Size Exclusion Chromatography	4.0	239.4	0.5	957.7	2.0	475.0	70.9	54.9

for strategies 1 and 2, respectively (Tables 2A and 2B).

There was a loss of 31.07% and 41.57% of yield after cation exchange chromatography (Table 2A). However, no enzymatic activity was detected in the column outlet during the loading, thus ruling out the possibility that the column was saturated protein. After adopting strategy 2 as a protocol, we evaluated the recovery and yield factor with the 30 and 100 kDa cassettes (Table 3).

We can conclude that the strategy with the highest yield for L-ASNase purification was strategy 2 using the 10 kDa diameter cut-off cassette (Table 3). Using the 100 kDa cassette we had the highest loss. Interestingly, using the 30 kDa cassette we obtained a lower yield, but also the highest purification factor among all the studied conditions.

In a study conducted by De Castro Girão and collaborators [34], a glycosylated L-ASNase obtained from *S. cerevisiae* was expressed in *P. pastoris*. The authors firstly employed size exclusion chromatography, and then ion-exchange chromatography (MONO-Q) (Table 4). A single active peak in molecular exclusion and 4 active peaks in cation exchange were obtained, which, according to the authors, were attributed to different proteoforms related to different post-translational modifications. The final yield of the process and the specific activity obtained were, respectively, 51.3% and 204.4 Umg^{-1} [34].

Lopes and coauthors [35] found an estimated weight for their L-ASNase of 178 kDa after gel filtration (Table 4). The final yield reached by the authors after affinity chromatography was 11.4% with a specific activity of 5.4 Umg^{-1} from a L-ASNase from *S. cerevisiae* expressed in *E. coli* [35].

Studies undertaken by Kante and collaborators [36] evaluated the production and purification of recombinant human asparaginase expressed in *E. coli* by crossflow filtration at different temperatures (22, 25, and 28 °C) and transmembrane pressures (12, 16, 20 and 25 psi). They reported that using 12 and 16 psi transmembrane pressure reached a process yield of 70% and 74%, respectively [36]. The recombinant human asparaginase was purified using cation exchange chromatography (SP-Sepharose FF) in gradient mode elution and resulted in a 51% yield and specific activity of 200 Umg^{-1} [36]. Their findings corroborate with our founding yield of 72.08% using 15 psi transmembrane pressure

Table 3
Evaluation of purification fold and final yield of the downstream process from the glycosylated L-ASNase through crossflow filtration using cassettes with variable cut-off sizes.

Cut off (kDa)	Purification fold	Final yield (%)
10 (strategy 1)	44.5	39.3
10 (strategy 2)	70.9	54.9
30 (strategy 2)	102.7	45.2
100 (strategy 2)	45.9	15.9

Table 4
Final yield and specific activity of different recombinant L-ASNase reported in the literature.

L-ASNase source	Purification Methodology	Specific activity (U/mg)	Final yield (%)	Reference
Saccharomyces cerevisiae expressed by *Pichia pastoris*	Cross flow filtration, size exclusion, anionic exchange	204.4	51.3	[34]
Saccharomyces cerevisiae expressed by *Escherichia coli*	Affinity chromatography	5.4	11.4	[35]
Escherichia coli	Cross flow filtration and cationic exchange	200.0	51.0	[36]
Bacillus lincheniformis	Cross flow filtration, precipitation, ionic exchange, size exclusion	697.1	33.0	[37]
Erwinia chrysanthemi expressed by *Escherichia coli*	Anionic exchange	312.8	17.8	[38]
Escherichia coli	Affinity chromatography	190.0	86.0	[39]
Escherichia coli	Anionic exchange and size exclusion	190.0	50.8	[40]
Erwinia chrysanthemi expressed by *Pichia pastoris*	Cross flow filtration, cationic exchange, size exclusion	475.0	54.9	This work

and the same membrane pore size 10 kDa as in the present study (Table 4).

Other studies reported the recovery of L-ASNase from *Bacillus lincheniformis* by ultrafiltration, reaching a 94.81% yield [37]. Since ultrafiltration is a process involving pressure action, the optimal transmembrane pressure (TMP) filtration operation is also very important to protect the protein's native structure. The lower recovery yield may be due to the formation of protein aggregates caused by the solution feed flow in the membrane with increasing pressure [36].

Trang and coauthors [38] studied the purification of L-ASNase from *E. chrysanthemi* expressed by *E. coli,* and after two chromatographic steps (Sephacryl and DEAE) the authors obtained a final yield of 17.8% with a specific activity of 312.8 Umg^{-1} [38]. Another study obtained an 86% of yield and a specific activity of 190 Umg^{-1} using affinity chromatography from an extracellularly L-ASNase expressed in *E. coli* [39].

Other studies employed anionic exchange chromatography (DEAE column) and size exclusion chromatography to purify a L-ASNase from *E. coli* and obtained 50.8% and 190 Umg^{-1} of final yield and specific activity [40].

Our findings had shown after cation exchange and size exclusion chromatography, we achieved a specific activity of 128.04 Umg^{-1}, 253.26 Umg^{-1}, respectively, and a yield of 56.63% and 54.93%, respectively. Table 4 summarizes the yield and specific activities reported in the literature from the purification process of other recombinant L-ASNase and in the present work.

3.4. Evaluation of the cytotoxicity activity of the glycosylated L-ASNase using a high throughput fluorescent-based platform

The anti-leukemic and anticancer effect of L-ASNases has been extensively investigated however, the effect of the recombinant glycosylated L-ASNase on human leukemic cells has not been fully elucidated. There is compelling evidence showing that the BM microenvironment can promote resistance to ASNases by secreting and providing Asn to leukemic cells [41] or through production of the protease cathepsin B, which inactivates ASNases [4]. Hence, the efficacious validation of efficacy of ASNases against leukemia cells requires the use of co-culture models that mimic as close as possible the in vivo setting. We used in our study the commonly used BM stromal cell line HS5 expressing mCherry, which closely recapitulates critical characteristics of the cytoprotective mesenchymal/fibroblastic BM niche [26,30,42]. To study the effect of purified recombinant L-ASNase on human leukemic cell lines, eGFP-tumour cells were cultured on their own and co-cultured with mCherry-HS5 (Fig. 4) and were treated with different concentrations of the purified enzyme.

Treatment with glycosylated L-ASNase resulted in the complete repression of the proliferation of all the cell lines under study from the lowest L-ASNase concentration tested (0.1 IU) independently of the presence of the BM stromal cell line mCherry-HS5 (Fig. 4). This is a valuable information considering that lower doses of glycosylated L-ASNase may required for the treatment turning more feasible the production of this biopharmaceutical in an industrial context of bioprocess and avoiding undesirable effects by the patient.

However, in terms of the impact of L-ASNase on cell viability we observed differences among cell lines. Glycosylated L-ASNase induced a concentration-dependent increase in the percentage of apoptotic cells in the ALL cell lines eGFP-SEMK2 and eGFP-REH (Fig. 4 B, E). A stronger cytotoxic effect of glycosylated L-ASNase was observed in eGFP- HB-119 cells cultured on its own and co-cultured with the BM stromal fibroblast cell line HS5 (Fig. 4 G, H, I). At the lowest concentration tested (0.1 IU), L-ASNase induced apoptosis in 100% of eGFP- HB-119 independently of the presence of BM stromal cells (Fig. 4 H). In contrast, the presence of mCherry-HS5 cells significantly inhibited the pro-apoptotic effect of L-ASNase in eGFP-SEMK2 and particularly, in eGFP-REH cells. Additionally, eGFP-REH showed the lowest levels of apoptosis in comparison to eGFP-SEMK2 and eGFP-HB-119 cells under all the experimental conditions tested (Fig. 4 A-L). In a recent study, different cell lines were tested against four different L-ASNase proteoforms. Although the study was conducted using the MTT methodology, it was also observed that the REH strain was the most resistant strain to the treatment with L-Asparaginase, while on the other hand, the MOLT-4 linage was the most sensitive to treatment [43]. This may be explained because the REH strain express lysosomal proteases, such as cathepsin B, that inactivate L-ASNase.

Interestingly, the AML eGFP-MV4–11 strain responded in a concentration-dependent manner to treatment with L-ASNase leading to apoptosis (Fig. 4 K). HS5 cells have been shown to inhibit the efficacy of clinical drugs against AML [44]. However, in our study the presence of HS5 cells failed to offer cytoprotection of eGFP-MV4–11 cells against L-ASNase. These results suggest that L-ASNase treatment may overcome resistance mediated by the BM mesenchymal/fibroblastic niche at least for some AML cells. Saeed and collaborators reported that their recombinant L-ASNase also presented cytotoxicity activity against the AML linage THP-1 [45]. As previously described by Michelozzi and collaborators [4] AML cells have variable expression of asparagine synthetase and seem susceptible to glutamine depletion. This explains why L-ASNase is not commonly used as first protocol in AML treatment. The authors evaluated the cytotoxicity activity of the commercial L-ASNases against THP-1, KG-1 and HL-60 [4]. Their findings showed a superior efficacy of Erwinase® in all AML cell lines tested in terms of induction of apoptosis rather than the *E. coli* ASNase (Kidrolase®) [4]. Furthermore, Emadi and co-authors found that Erwinase showed anti-leukemic afficacy as a single agent in two out five AML patients studied [46]. All these findings support that our recombinant glycosilated L-ASNase may also be used to treat AML disorder since it is the same protein expressed by *Erwinia chrysanthemi* with human-like glycosylation patterns added by *Pichia pastoris*.

It is noterworthy that glycosylated L-ASNase also induced a significant inhibition of the proliferation of HS5 fibroblast cells (Fig. 4 M). Since the HS5 stromal cell are source of L-asparagine for leukemic blasts, this repression of the activity of thi cytoprotective BM niche by L-ASNase may represent a mechanism of action of glycosylated L-ASNases by interfering with the BM tumour microenvironment avoiding cytoprotection and relapse of the disease.

Taken together, our data show that glycosylated L-ASNase shows high cytostatic and cytotoxic activity against ALL and AML cells and interferes with the possible expansion of cytoprotective BM mesenchymal/fibroblastic cells. Overall, our results indicate high efficacy of glycosylated ASNase against ALL and possibly AML, albeit with different degrees of impact depending on the capacity of leukemia cells to stimulate the interaction with cytoprotective BM stromal niches.

3.5. Effect of L-ASNase treatment in the leukemic cells intracellular aminoacids

Chiu and collaborators proposed an amino acid trade-off mechanism to explain the resistance against L-ASNase along the treatment [41]. According to the authors, stromal cells adapt to L-ASNase and protect leukemic blasts from the enzyme action. The leukemic blasts synthesize and secrete glutamine, increasing the extracellular glutamine availability, which is used by stromal cells to synthetize asparagine, which is then released to keep the asparagine-auxotrophic leukemic blasts. Considering this mechaminism, the inhibition of glutaminase syntetase by L-ASNase avoids this trade-off mechanism.

Thus, in order to evaluate the nutritional support interplayed between stromal cells and leukemic blasts, an intracellular amino acids analysis was performed after the treatment with the glycosylated L-ASNase. For those tests, we selected the concentration of 0.3 IU and cell cultures were treated for 24 h, and we identified the intracellular metabolites by UPLC-MS/MS in the HB-119, REH and MV4–11 lineages (Fig. 5).

Upon L-Asparaginase treatment, we detected a major decrease in

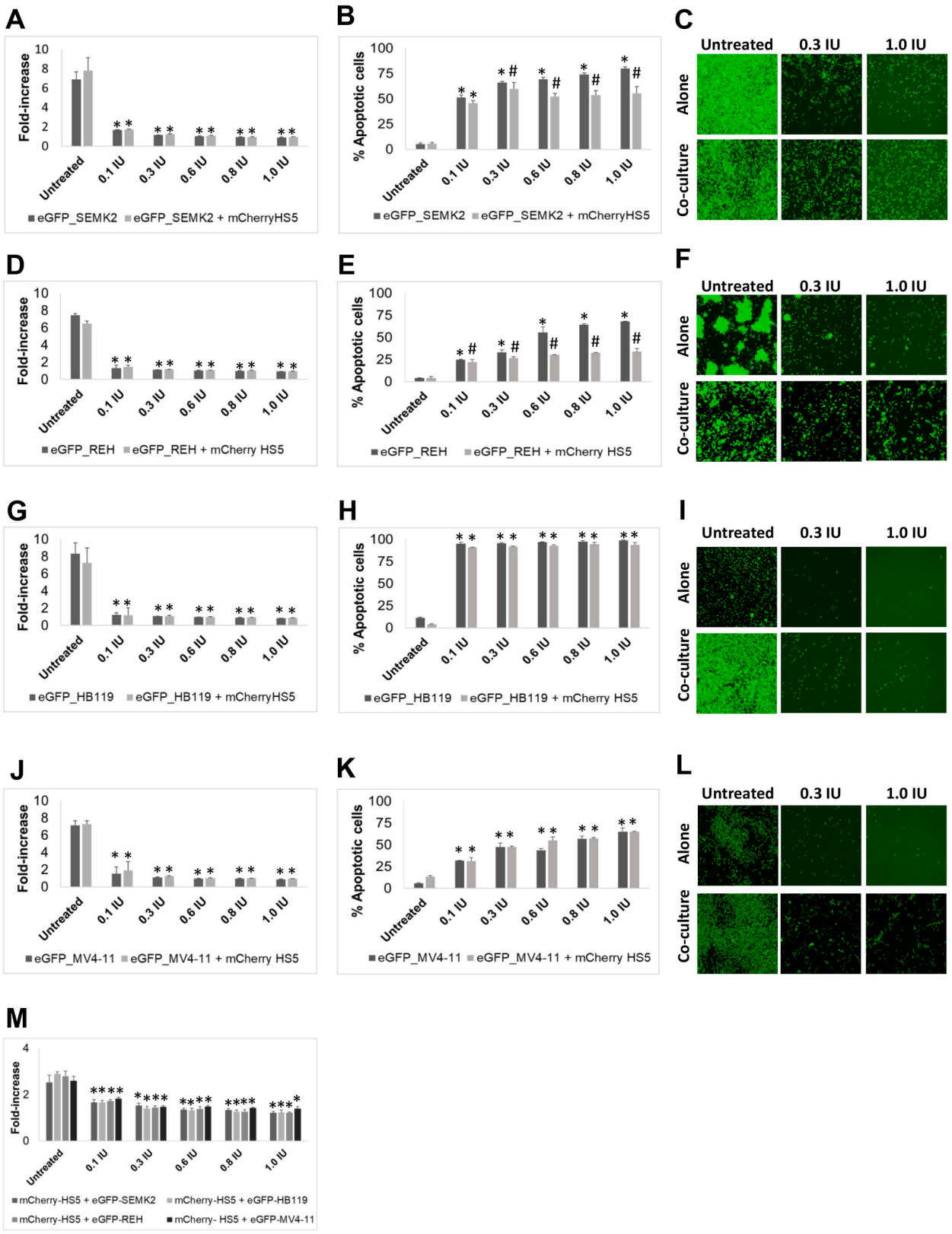

Fig. 4. Analysis of the impact of glycosylated L-ASNase on tumour and stromal cell proliferation in co-culture. Fluorescent-based analysis of proliferation of eGFP-expressing leukemic cell lines (A, D, G, J) and mCherry-expressing HS5 stromal cells (M) in response to increasign concentrations of glycosylated L-ASNase. Proliferation of cells was evaluated after 72 h. Percentage of apoptotic cells in response to glycosylated L-ASNase treatment (B, E, H, K) analysed by FACS. Fluorescence micrographs showing the presence of eGFP-SEMK2 cells (C), eGFP-REH cells (F), eGFP-HB-119 cells (I) and eGFP-MV4–11 cells (L) cultured alone or in the presence of mCherry-HS5 BM stromal cells. All experiments were repeated 3 times.*$P < 0.001$, ANOVA test *versus* control (untreated). #$P < 0.001$ ANOVA test *versus* co-coltured models.

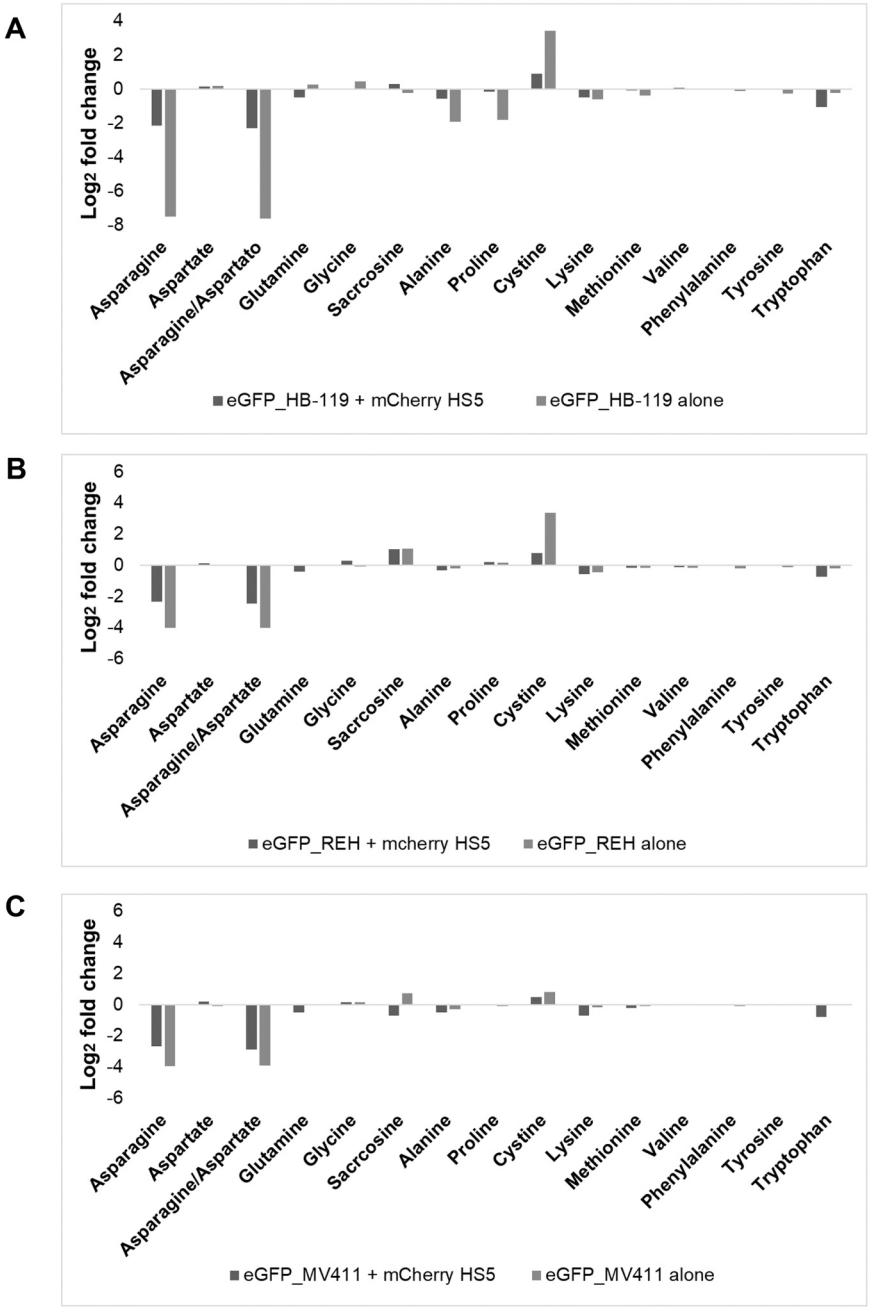

Fig. 5. Comparison of the content of intracellular metabolites identified by UPLC-MS/MS after 24 h of the treatment with the glycosylated L-ASNase. Graphs show absolute levels of each metabolite. The recombinant L-ASNase depletes asparagine when tumour cells are culture on their own, however, in the presence of BM stromal cells it is possible to detect asparagine suggesting that the tumour microenvironment influences the response to chemotherapy. L-ASNse concentration: 0.3 IU. Leukemic cell lines evaluated: A) HB-119 B) REH and C) MV411.

intracellular asparagine levels when tumour cells were cultured on their own. In contrast, when tumour cells were co-cultured with stromal cells, all leukemia cell lines tested sustained higher levels of intracellular asparagine (Fig. 5). These data reaffirm that BM provides cytoprotection to tumour cells by synthesizing and providing asparagine [41]. In contrast, the levels of glutamine did not fluctuate with treatment with glycosylated L-ASNase, indicating a high specificity of the enzyme for asparagine. In comparison, some previously reported ASNases have demonstrated low specificity as they also show glutaminase activity [43], which may results in unwated side effects on healthy tissues.

In addition, the highest concentration of lysine for all three cell lines studied was detected when the tumour cells were co-cultured with BM. These result suggests a possible dependence by cancer cells of lysine synthesized by BM stromal cells, which could potentially lead to future drug discovery studies targeting also lysine [47]. It is also important to remark that from the lysine perspective, we can see a difference in the response between ALL and AML cells. When MV4–11 cells were cultured alone, treatment with glycosylated L-ASNase had a minor impact on the levels of lysine whereas a significant reduction in lysine levels were observed in the two ALL cell lines tested under the same experimental conditions.

4. Conclusion

In summary, the recombinant glycosylated L-ASNase generated in this study induced a cytotoxic effect in all human leukemic cell lines tested. These data support the potential of the glycosylated L-ASNase as a promising alternative enzyme in ALL treatment and warrants further studies to explore its application against AML treatment as well. The method described for L-ASNase purification may be used for the development of a further bioprocess to better address the challenge of offering alternative L-ASNase with high purity and yield. In addition, our data

show the critical role of the cytoprotection of ALL and AML cells mediated by their interaction with BM stromal cell that should be taken into consideration for any significant pre-clinical investigations to study the efficacy of L-ASNases.

CRediT authorship contribution statement

EKK, YC and **AP** designed the research. **EKK** designed and performed experiments, analysed the results, made the related figures. **EKK** and **YC** wrote the manuscript. **YAB** generated the **eGFP-AML** and **eGFP-ALL** cell lines. **LAP** and **BE** helped with protein expression and purification. **PFL** helped with proteomics analysis. **AP, YC, MTE** and **VB** participated in the supervision of the project. **YC, GM, MTE, VB**, **YAB** and **AP** reviewed and edited the paper. **AP, GM** and **YC** provided financial support for the research.

Declaration of Competing Interest

We, Yolanda Calle and Eduardo Krebs Kleingesinds– corresponding authors, on behalf of all authors disclose that we do not have any financial and personal relationships with other people or organizations that could inappropriately influenced (bias) this work.

Data Availability

No data was used for the research described in the article.

Acknowledgments

This work was financially supported by FAPESP (grant numbers 2013/08617–7, 2015/07749–2, 2017/20384–9, 2017/25065–9, 2018/15104–0, 2018/03734–9, 2019/06919–2); the Comisión Nacional de Investigación Científica y Tecnológica (CONICYT/Chile) [21150288]; Agencia Nacional de Investigación y Desarrollo (ANID) Fondecyt de postdoctorado Folio 3210142; DI12-PEO1 [EXE12–0004] DIUFRO and CAPES (finance code 001), a Brazilian research agency. GM received the researcher productivity fellowship 309224/2019–5 from CNPq. YC received funding from Cancer Research UK (reference C34579/A20784).

References

[1] B. Lopez-Millan, D. Sanchéz-Martínez, H. Roca-Ho, F. Gutiérrez-Agüera, O. Molina, R. Diaz de la Guardia, R. Torres-Ruiz, J.L. Fuster, P. Ballerini, U. Suessbier, C. Nombela-Arrieta, C. Bueno, P. Menéndez, NG2 antigen is a therapeutic target for MLL-rearranged B-cell acute lymphoblastic leukemia, Leukemia 33 (2019) 1557–1569, https://doi.org/10.1038/s41375-018-0353-0.

[2] L.P. Brumano, F.V.S. da Silva, T.A. Costa-Silva, A.C. Apolinário, J.H.P.M. Santos, E. K. Kleingesinds, G. Monteiro, C. de, O. Rangel-Yagui, B. Benyahia, A.P. Junior, Development of L-asparaginase biobetters: current research status and review of the desirable quality profiles, Front. Bioeng. Biotechnol. 6 (2019), https://doi.org/10.3389/fbioe.2018.00212.

[3] K.S. Siveen, S. Uddin, R.M. Mohammad, Targeting acute myeloid leukemia stem cell signaling by natural products, Mol. Cancer 16 (2017), https://doi.org/10.1186/s12943-016-0571-x.

[4] I.M. Michelozzi, V. Granata, G. De Ponti, G. Alberti, C. Tomasoni, L. Antolini, C. Gambacorti-Passerini, B. Gentner, F. Dazzi, A. Biondi, T. Coliva, C. Rizzari, A. Pievani, M. Serafini, Acute myeloid leukaemia niche regulates response to L-asparaginase, Br. J. Haematol. 186 (2019) 420–430, https://doi.org/10.1111/bjh.15920.

[5] C. Korn, S. Méndez-Ferrer, Myeloid malignancies and the microenvironment, Blood 129 (2017) 811–822, https://doi.org/10.1182/blood-2016-09-670224.

[6] Q. Heydt, C. Xintaropoulou, A. Clear, M. Austin, I. Pislariu, F. Miraki-Moud, P. Cutillas, K. Korfi, M. Calaminici, W. Cawthorn, K. Suchacki, A. Nagano, J. G. Gribben, M. Smith, J.D. Cavenagh, H. Oakervee, A. Castleton, D. Taussig, B. Peck, A. Wilczynska, L. McNaughton, D. Bonnet, F. Mardakheh, B. Patel, Adipocytes disrupt the translational programme of acute lymphoblastic leukaemia to favour tumour survival and persistence, Nat. Commun. 12 (2021) 5507, https://doi.org/10.1038/s41467-021-25540-4.

[7] M. Steiner, D. Hochreiter, D.C. Kasper, R. Kornmüller, H. Pichler, O.A. Haas, U. Pötschger, C. Hutter, M.N. Dworzak, G. Mann, A. Attarbaschi, Asparagine and aspartic acid concentrations in bone marrow versus peripheral blood during Berlin-Frankfurt-Münster-based induction therapy for childhood acute lymphoblastic leukemia, Leuk. Lymphoma 53 (2012) 1682–1687, https://doi.org/10.3109/10428194.2012.668681.

[8] J. Nomme, Y. Su, M. Konrad, A. Lavie, Structures of apo and product-bound human L-asparaginase: insights into the mechanism of autoproteolysis and substrate hydrolysis, Biochemistry 51 (2012) 6816–6826, https://doi.org/10.1021/bi300870g.

[9] N. Patel, S. Krishnan, M.N. Offman, M. Krol, C.X. Moss, C. Leighton, F.W. van Delft, M. Holland, J. Liu, S. Alexander, C. Dempsey, H. Ariffin, M. Essink, T.O. Eden, C. Watts, P.A. Bates, V. Saha, A dyad of lymphoblastic lysosomal cysteine proteases degrades the antileukemic drug L-asparaginase, J. Clin. Invest 119 (2009) 1964–1973, https://doi.org/10.1172/JCI37977.

[10] L.T. van der Meer, E. Waanders, M. Levers, H. Venselaar, D. Roeleveld, J. Boos, C. Lanvers, R.J. Brüggemann, R.P. Kuiper, P.M. Hoogerbrugge, F.N. van Leeuwen, D.M. Loo, A germ line mutation in cathepsin B points toward a role in asparaginase pharmacokinetics, Blood 124 (2014) 3027–3029, https://doi.org/10.1182/blood-2014-06-582627.

[11] B. Effer, E.K. Kleingesinds, G.M. Lima, I.M. Costa, I. Sánchez-Moguel, A. Pessoa, V. F. Santiago, G. Palmisano, J.G. Farías, G. Monteiro, Glycosylation of Erwinase results in active protein less recognized by antibodies, Biochem. Eng. J. 163 (2020), 107750, https://doi.org/10.1016/j.bej.2020.107750.

[12] T.A. Costa-Silva, I.M. Costa, H.P. Biasoto, G.M. Lima, C. Silva, A. Pessoa, G. Monteiro, Critical overview of the main features and techniques used for the evaluation of the clinical applicability of L-asparaginase as a biopharmaceutical to treat blood cancer, Blood Rev. 43 (2020), 100651, https://doi.org/10.1016/j.blre.2020.100651.

[13] A.C. Apolinário, M.S. Magoń, A. Pessoa, C. de, O. Rangel-Yagui, Challenges for the self-assembly of poly(Ethylene glycol)-poly(lactic acid) (PEG-PLA) into polymersomes: beyond the theoretical paradigms, Nanomaterials 8 (2018) 373, https://doi.org/10.3390/nano8060373.

[14] K. Torres-Obreque, G.P. Meneguetti, D. Custódio, G. Monteiro, A. Pessoa-Junior, C. de Oliveira Rangel-Yagui, Production of a novel N-terminal PEGylated crisantaspase, Biotechnol. Appl. Biochem. 66 (2019) 281–289, https://doi.org/10.1002/bab.1723.

[15] G.P. Meneguetti, J.H.P.M. Santos, K.M.T. Obreque, C.M.V. Barbosa, G. Monteiro, S. H.P. Farsky, A.M. Oliveira, C.B. Angeli, G. Palmisano, S.P.M. Ventura, A. Pessoa-Junior, C.O. Rangel-Yagui, Novel site-specific PEGylated L-asparaginase, Plos One 14 (2019), e0211951, https://doi.org/10.1371/journal.pone.0211951.

[16] W. Vervecken, V. Kaigorodov, N. Callewaert, S. Geysens, K. De Vusser, R. Contreras, *In vivo* synthesis of mammalian-like, hybrid-type N-glycans in *Pichia pastoris*, Appl. Environ. Microbiol. 70 (2004) 2639–2646, https://doi.org/10.1128/AEM.70.5.2639-2646.

[17] D. Skropeta, The effect of individual N-glycans on enzyme activity, Bioorg. Med. Chem. 17 (2009) 2645–2653, https://doi.org/10.1016/j.bmc.2009.02.037.

[18] K. De Pourcq, K. De Schutter, N. Callewaert, Engineering of glycosylation in yeast and other fungi: current state and perspectives, Appl. Microbiol. Biotechnol. 87 (2010) 1617–1631, https://doi.org/10.1007/s00253-010-2721-1.

[19] D. Hopkins, S. Gomathinayagam, A.M. Rittenhour, M. Du, E. Hoyt, K. Karaveg, T. Mitchell, J.H. Nett, N.J. Sharkey, T.A. Stadheim, H. Li, S.R. Hamilton, Elimination of β-mannose glycan structures in *Pichia pastoris*, Glycobiology 21 (2011) 1616–1626, https://doi.org/10.1093/glycob/cwr108.

[20] C.M. Zwaan, G.J. Kaspers, R. Pieters, N.L. Ramakers-Van Woerden, M.L. den Boer, R. Wünsche, M.M. Rottier, K. Hählen, E.R. van Wering, G.E. Janka-Schaub, U. Creutzig, A.J. Veerman, Cellular drug resistance profiles in childhood acute myeloid leukemia: differences between FAB types and comparison with acute lymphoblastic leukemia, Blood 96 (2000) 2879–2886, https://doi.org/10.1182/blood.V96.8.2879.

[21] S. Okada, T. Hongo, S. Yamada, C. Watanabe, Y. Fujii, T. Ohzeki, Y. Horikoshi, T. Ito, M. Yazaki, Y. Komada, A. Tawa, *In vitro* efficacy of L-asparaginase in childhood acute myeloid leukaemia, Br. J. Haematol. 123 (2003) 802–809, https://doi.org/10.1046/j.1365-2141.2003.04703.x.

[22] S.N. Bertuccio, S. Serravalle, A. Astolfi, A. Lonetti, V. Indio, A. Leszl, A. Pession, F. Melchionda, Identification of a cytogenetic and molecular subgroup of acute myeloid leukemias showing sensitivity to L-Asparaginase, Oncotarget 8 (2017) 109915–109923, https://doi.org/10.18632/oncotarget.18565.

[23] L. Willems, N. Jacque, A. Jacquel, N. Neveux, T.T. Maciel, M. Lambert, A. Schmitt, L. Poulain, A.S. Green, M. Uzunov, O. Kosmider, I. Radford-Weiss, I.C. Moura, P. Auberger, N. Ifrah, V. Bardet, N. Chapuis, C. Lacombe, P. Mayeux, J. Tamburini, D. Bouscary, Inhibiting glutamine uptake represents an attractive new strategy for treating acute myeloid leukemia, Blood 122 (2013) 3521–3532, https://doi.org/10.1182/blood-2013-03-493163.

[24] N. Jacque, A.M. Ronchetti, C. Larrue, G. Meunier, R. Birsen, L. Willems, E. Saland, J. Decroocq, T.T. Maciel, M. Lambert, L. Poulain, M.A. Hospital, P. Sujobert, L. Joseph, N. Chapuis, C. Lacombe, I.C. Moura, S. Demo, J.E. Sarry, C. Recher, P. Mayeux, J. Tamburini, D. Bouscary, Targeting glutaminolysis has antileukemic activity in acute myeloid leukemia and synergizes with BCL-2 inhibition, Blood 126 (2015) 1346–1356, https://doi.org/10.1182/blood-2015-01-621870.

[25] P. Matre, J. Velez, R. Jacamo, Y. Qi, X. Su, T. Cai, S.M. Chan, A. Lodi, S.R. Sweeney, H. Ma, R.E. Davis, N. Baran, T. Haferlach, X. Su, E.R. Flores, D. Gonzalez, S. Konoplev, I. Samudio, C. DiNardo, R. Majeti, A.D. Schimmer, W. Li, T. Wang, S. Tiziani, M. Konopleva, Inhibiting glutaminase in acute myeloid leukemia: metabolic dependency of selected AML subtypes, Oncotarget 7 (2016) 79722–79735, https://doi.org/10.18632/oncotarget.12944.

[26] K. Ramasamy, H. Khatun, L. Macpherson, M.P. Caley, J. Sturge, G.J. Mufti, S. A. Schey, Y. Calle, Fluorescence-based experimental model to evaluate the concomitant effect of drugs on the tumour microenvironment and cancer cells, Br.

J. Haematol. 157 (2012) 564–579, https://doi.org/10.1111/j.1365-2141.2012.09103.x.
[27] B. Effer, G. Meira, S. Cabarca, A. Pessoa, J. Farias, G. Monteiro, L-asparaginase from *E. chrysamthemi* expressed in Glycoswitch: Effect of His-tagg fusion on the extracellular expression, Prep. Biochem. Biotechnol. 49 (2019) 679–685, https://doi.org/10.1080/10826068.2019.1599396.
[28] L.A. Parizotto, E.K. Kleingesinds, L.M.P. Rosa, B. Effer, G.M. Lima, M. E. Herkenhoff, Z. Li, U. Rinas, G. Monteiro, A. Pessoa, A. Tonso, Increased glycosylated l-asparaginase production through selection of *Pichia pastoris* platform and oxygen-methanol control in fed-batches, Biochem. Eng. J. 173 (2021), 108083, https://doi.org/10.1016/j.bej.2021.108083.
[29] R.G. Simas, E.K. Kleingesinds, A. Pessoa, P.F. Long, An improved method for simple and accurate colorimetric determination of l-asparaginase enzyme activity using Nessler's reagent, J. Chem. Technol. Biotechnol. 96 (2021) 1326–1332, https://doi.org/10.1002/jctb.6651.
[30] Y. Arroyo-Berdugo, M. Sendino, D. Greaves, N. Nojszewska, O. Idilli, C.W. So, L. Di Silvio, R. Quartey-Papafio, F. Farzaneh, J.A. Rodriguez, Y. Calle, High throughput fluorescence-based *In Vitro* experimental platform for the identification of effective therapies to overcome tumour microenvironment mediated drug resistance in AML, Cancers 15 (2023) 1988, https://doi.org/10.3390/cancers15071988.
[31] N. Gray, R. Zia, A. King, V.C. Patel, J. Wendon, M.J. McPhail, M. Coen, R.S. Plumb, I.D. Wilson, J.K. Nicholson, High-speed quantitative UPLC-MS analysis of multiple amines in human plasma and serum via precolumn derivatization with 6-amino-quinolyl-n-hydroxysuccinimidyl carbamate: application to acetaminophen-induced liver failure, Anal. Chem. 89 (2017) 2478–2487, https://doi.org/10.1021/acs.analchem.6b04623.
[32] S.K. Niazi, The coming of age of biosimilars: a personal perspective, Biologics 2 (2022) 107–127, https://doi.org/10.3390/biologics2020009.
[33] P.P. Zenatti, N.A. Migita, N.M. Cury, R.A. Mendes-Silva, F.C. Gozzo, P.O. de Campos-Lima, J.A. Yunes, S.R. Brandalise, Low bioavailability and high immunogenicity of a new brand of *E. coli* L-asparaginase with active host contaminating proteins, EBioMedicine 30 (2018) 158–166, https://doi.org/10.1016/j.ebiom.2018.03.005.
[34] L.F. De Castro Girão, S.L.G. Da Rocha, R.S. Sobral, A.P. Dinis Ano Bom, A.L. Franco Sampaio, J.G. Da Silva, M.A. Ferrara, E.P. Da Silva Bon, J. Perales, *Saccharomyces cerevisiae* asparaginase II, a potential antileukemic drug: Purification and characterization of the enzyme expressed in Pichia pastoris, Protein Expr. Purif. 120 (2016) 118–125, https://doi.org/10.1016/j.pep.2015.12.012.
[35] W. Lopes, B.A.F. dos Santos, A.L.F. Sampaio, A.P. Gregório Alves Fontão, H. J. Nascimento, P.B. Jurgilas, F.A.G. Torres, E.P. da, S. Bon, R.V. Almeida, M. A. Ferrara, Expression, purification, and characterization of asparaginase II from *Saccharomyces cerevisiae* in *Escherichia coli*, Protein Expr. Purif. 159 (2019) 21–26, https://doi.org/10.1016/j.pep.2019.02.012.
[36] R.K. Kante, S. Vemula, S. Somavarapu, M.R. Mallu, B.H. Boje Gowd, S.R. Ronda, Optimized upstream and downstream process conditions for the improved production of recombinant human asparaginase (rhASP) from *Escherichia coli* and its characterization, Biologics 56 (2018) 45–53, https://doi.org/10.1016/j.biologicals.2018.10.002.
[37] R.V. Mahajan, V. Kumar, V. Rajendran, S. Saran, P.C. Ghosh, R.K. Saxena, Purification and characterization of a novel and robust L-asparaginase having low-glutaminase activity from *Bacillus licheniformis*: *In vitro* evaluation of anti-cancerous properties, PLoS One 9 (2014), e99037, https://doi.org/10.1371/journal.pone.0099037.
[38] T.H.N. Trang, T.N. Cuong, S.L.N. Thanh, T. Do Tuyen, Optimization, purification and characterization of recombinant L-asparaginase II in *Escherichia coli*, Afr. J. Biotechnol. 15 (2016) 1681–1691, https://doi.org/10.5897/ajb2016.15425.
[39] A. Khushoo, Y. Pal, B.N. Singh, K.J. Mukherjee, Extracellular expression and single step purification of recombinant *Escherichia coli* l-asparaginase II, Protein Expr. Purif. 38 (2004) 29–36, https://doi.org/10.1016/j.pep.2004.07.009.
[40] A.K. Upadhyay, A. Singh, K.J. Mukherjee, A.K. Panda, Refolding and purification of recombinant L-asparaginase from inclusion bodies of *E. coli* into Act. tetrameric Protein, Front. Microbiol 5 (2014) 1–10, https://doi.org/10.3389/fmicb.2014.00486.
[41] M. Chiu, G. Taurino, E. Dander, D. Bardelli, A. Fallati, R. Andreoli, M.G. Bianchi, C. Carubbi, G. Pozzi, L. Galuppo, P. Mirandola, C. Rizzari, S. Tardito, A. Biondi, G. D'Amico, O. Bussolati, ALL blasts drive primary mesenchymal stromal cells to increase asparagine availability during asparaginase treatment, Blood Adv. 5 (2021) 5164–5178, https://doi.org/10.1182/bloodadvances.2020004041.
[42] D.W. McMillin, J. Delmore, E. Weisberg, J.M. Negri, D.C. Geer, S. Klippel, N. Mitsiades, R.L. Schlossman, N.C. Munshi, A.L. Kung, J.D. Griffin, P. G. Richardson, K.C. Anderson, C.S. Mitsiades, Tumor cell-specific bioluminescence platform to identify stroma-induced changes to anticancer drug activity, Nat. Med. 16 (2010) 483–489, https://doi.org/10.1038/nm.2112.
[43] M.A.D. Rodrigues, M.V. Pimenta, I.M. Costa, P.P. Zenatti, N.A. Migita, J.A. Yunes, C.O. Rangel-Yagui, M.M. de Sá, A. Pessoa, T.A. Costa-Silva, M.H. Toyama, C. A. Breyer, M.A. de Oliveira, V.F. Santiago, G. Palmisano, C.M.V. Barbosa, C. B. Hebeda, S.H.P. Farsky, G. Monteiro, Influence of lysosomal protease sensitivity in the immunogenicity of the antitumor biopharmaceutical asparaginase, Biochem. Pharmacol. 182 (2020), 114230, https://doi.org/10.1016/j.bcp.2020.114230.
[44] S.M. Garrido, F.R. Appelbaum, C.L. Willman, D.E. Banker, Acute myeloid leukemia cells are protected from spontaneous and drug-induced apoptosis by direct contact with a human bone marrow stromal cell line (HS-5, Exp. Hematol. 29 (2001) 448–457, https://doi.org/10.1016/s0301-472x(01)00612-9.
[45] H. Saeed, A. Hemida, N. El-Nikhely, M. Abdel-Fattah, M. Shalaby, A. Hussein, A. Eldoksh, F. Ataya, N. Aly, N. Labrou, H. Nematalla, Highly efficient *Pyrococcus furiosus* recombinant L-asparaginase with no glutaminase activity: expression, purification, functional characterization, and cytotoxicity on THP-1, A549 and Caco-2 cell lines, Int. J. Biol. Macromol. 156 (2020) 812–828, https://doi.org/10.1016/j.ijbiomac.2020.04.080.
[46] A. Emadi, J.Y. Law, E.T. Strovel, R.G. Lapidus, L.J.B. Jeng, M. Lee, M.G. Blitzer, B. A. Carter-Cooper, D. Sewell, I. van der Merwe, S. Philip, M. Imran, S.L. Yu, H. Li, P. C. Amrein, V.H. Duong, E.A. Sausville, M.R. Baer, A.T. Fathi, Z. Singh, S. M. Bentzen, Asparaginase *Erwinia chrysanthemi* effectively depletes plasma glutamine in adult patients with relapsed/refractory acute myeloid leukemia, Cancer Chemother. Pharmacol. 81 (2018) 217–222, https://doi.org/10.1007/s00280-017-3459-6.
[47] V.S. Pokrovsky, L. Abo Qoura, E. Morozova, Bunik VI. Predictive markers for efficiency of the amino-acid deprivation therapies in cancer, Front. Med 9 (2022) 1035356, https://doi.org/10.3389/fmed.2022.1035356.